

Formation of patterned ground and sublimation till over Miocene glacier ice in Beacon Valley, southern Victoria Land, Antarctica

D.R. Marchant*

A.R. Lewis

Department of Earth Sciences, Boston University, Boston, Massachusetts 02215, USA

W.M. Phillips

Department of Geography, University of Edinburgh, Edinburgh EH8 9XP, UK

E.J. Moore

Department of Earth Sciences, Boston University, Boston, Massachusetts 02215, USA

R.A. Souchez

Département des Sciences de la Terre et de l'Environnement, CP 160/03, Université Libre de Bruxelles, B-1050 Bruxelles, Belgium

G.H. Denton

Department of Geological Sciences and Institute for Quaternary Studies, University of Maine, Orono, Maine 04469, USA

D.E. Sugden

Department of Geography, University of Edinburgh, Edinburgh EH8 9XP, UK

N. Potter Jr.

Department of Geology, Dickinson College, Carlisle, Pennsylvania 17013, USA

G.P. Landis

U.S. Geological Survey, Denver Federal Center, Denver, Colorado 80225, USA

ABSTRACT

A thin glacial diamicton, informally termed Granite drift, occupies the floor of central Beacon Valley in southern Victoria Land, Antarctica. This drift is <1.0 m thick and rests with sharp planar contacts on stagnant glacier ice reportedly of Miocene age, older than 8.1 Ma. The age of the ice is based on $^{40}\text{Ar}/^{39}\text{Ar}$ analyses of presumed in situ ash-fall deposits that occur within Granite drift. At odds with the great age of this ice are high-centered polygons that cut Granite drift. If polygon development has reworked and retransported ash-fall deposits, then they are untenable as chronostratigraphic markers and cannot be used to place a minimum age on the underlying glacier ice.

Our results show that the surface of Granite drift is stable at polygon centers and that enclosed ash-fall deposits can be used to define the age of underlying glacier ice. In our model for patterned-ground development, active regions lie only above polygon troughs, where enhanced sublimation of underlying ice outlines high-centered polygons. The rate of sublimation is influenced by the development of porous gravel-and-cobble lag deposits that form above thermal-contraction cracks in the underlying ice. A negative feed-

back associated with the development of secondary-ice lenses at the base of polygon troughs prevents runaway ice loss. Secondary-ice lenses contrast markedly with glacial ice by lying on a δD versus $\delta^{18}\text{O}$ slope of 5 rather than a precipitation slope of 8 and by possessing a strongly negative deuterium excess. The latter indicates that secondary-ice lenses likely formed by melting, downward percolation, and subsequent refreezing of snow trapped preferentially in deep polygon troughs.

The internal stratigraphy of Granite drift is related to the formation of surface polygons and surrounding troughs. The drift is composed of two facies: A nonweathered, matrix-supported diamicton that contains >25% striated clasts in the >16 mm fraction and a weathered, clast-supported diamicton with varnished and wind-faceted gravels and cobbles. The weathered facies is a coarse-grained lag of Granite drift that occurs at the base of polygon troughs and in lenses within the nonweathered facies. The concentration of cosmogenic ^3He in dolerite cobbles from two profiles through the nonweathered drift facies exhibits steadily decreasing values and shows the drift to have formed by sublimation of underlying ice. These profile patterns and the ^3He surface-exposure ages of 1.18 ± 0.08 Ma and 0.18 ± 0.01 Ma atop these profiles indicate that churning of clasts by cryoturbation has not occurred at these sites in at least the past 10^5 and 10^6 yr. Although Granite

*E-mail: marchant@bu.edu.

drift is stable at polygon centers, low-frequency slump events occur at the margin of active polygons. Slumping, together with weathering of surface clasts, creates the large range of cosmogenic-nuclide surface-exposure ages observed for Granite drift. Maximum rates of sublimation near active thermal-contraction cracks, calculated by using the two ^3He depth profiles, range from 5 m/m.y. to 90 m/m.y. Sublimation rates are likely highest immediately following major slump events and decrease thereafter to values well below our maximum estimates. Nevertheless, these rates are orders of magnitude lower than those computed on theoretical grounds. During eruptions of the nearby McMurdo Group volcanic centers, ash-fall debris collects at the surface of Granite drift, either in open thermal-contraction cracks or in deep troughs that lie above contraction cracks; these deposits subsequently lower passively as the underlying glacier ice sublimates. The fact that some regions of Granite drift have escaped modification by patterned ground for at least 8.1 Ma indicates long-term geomorphic stability of individual polygons. Once established, polygon toughs likely persist for as long as 10^5 – 10^6 yr. Our model of patterned-ground formation, which applies to the hyperarid, cold-desert, polar climate of Antarctica, may also apply to similar-sized polygons on Mars that occur over buried ice in Utopia Planitia.

Keywords: Antarctica, cosmogenic-nuclide exposure dating, Dry Valleys, periglacial features, polygons.

INTRODUCTION

The age, distribution, and texture of glacial drifts in the Dry Valleys region of southern Victoria Land have long been used to decipher Antarctic paleoclimate (Denton et al., 1971, 1993). Near the coast, some late Wisconsinan drifts <1 m thick still retain a core of original glacier ice, providing strong evidence for cold-desert conditions throughout the Holocene (Stuiver et al., 1981; Denton et al., 1989; Denton and Marchant, 2000). Sugden et al. (1995) have suggested that a Miocene drift (older than 8.1 Ma) likewise retains its core of glacier ice in central Beacon Valley. $^{40}\text{Ar}/^{39}\text{Ar}$ analyses of single volcanic crystals within presumed in situ air-fall ash deposits within the drift provide geochronologic control (Sugden et al., 1995). If glacier ice can survive beneath a thin drift for up to 8.1 m.y. in central Beacon Valley, then cold-desert conditions in the Dry Valleys region must have persisted since at least late Miocene time (Sugden et al., 1995). Further, it opens up the possibility of retrieving pristine samples of Miocene atmosphere from gas in sealed bubbles in the ancient glacier ice.

One persistent and vexing problem that complicates direct dating of the buried ice in Beacon Valley is that its overlying drift shows well-developed surface polygons. These polygons imply that the drift is dynamic and likely undergoing near-surface convection with diapirism at polygon centers, diverging surface flow toward troughs, and sub-surface return flow to polygon centers (e.g., Hallet and Prestrud, 1986; Hallet and Waddington, 1991; Swanson et al., 1999). If the drift atop the buried ice is convecting, then enclosed ash-fall deposits have been reworked and are untenable as chronostratigraphic markers. In this paper, we reexamine the problem of the age and origin of the ancient glacier ice in Beacon Valley by investigating the development of its overlying till cover and associated patterned ground. Two key questions confront us: (1) Are the surface polygons in Beacon Valley produced through near-surface convection? (2) How do the polygons influence sublimation of the underlying glacier ice?

Physical Setting

Beacon Valley ($77^{\circ}50'\text{S}$, $159^{\circ}30'\text{E}$) is predominantly free of surface ice and lies at an average elevation of 1350 m (Fig. 1). The valley is situated at the center of the sandstone-and-dolerite-capped Quartermain Mountains. It is nearly 18 km in length and ranges from 2 to 3 km in width (Fig. 1). The bedrock consists of Devonian–Triassic sandstones, siltstones, and conglomerates of the Beacon Supergroup and Jurassic sills and dikes of Ferrar Dolerite (Barrett, 1981). There are few published reports for climate conditions of Beacon Valley, but measurements by Ugolini et al. (1971) taken during the austral summers of 1969–1970 and 1971–1972 indicate temperatures between -8°C and -14°C during the first weeks of November. On the basis of a recorded mean-annual temperature of about -19.8°C at ~ 100 m elevation at nearby Lake Vanda (Schwerdtfeger, 1984) and an average lapse rate of $1^{\circ}\text{C}/100$ m, we infer that the mean annual temperature in Beacon Valley is about -34°C . Local precipitation is probably <10 mm water equivalent per year (Schwerdtfeger, 1984). Soil temperatures, obtained for one calendar year in 1994 at 1600 m elevation in the nearby (~ 30 km) western Asgard Range (McKay et al., 1998) remained below 0°C at the surface and below -8°C at 17 cm depth (reaching a minimum of -40°C at 17 cm depth). We suggest that soil temperatures in central Beacon Valley, though not necessarily soil properties (Bockheim, 1990), are generally similar to those of the western Asgard Range. The soils of Beacon Valley and those measured in the western Asgard Range share similar geomorphic settings.

Outlet glaciers that drain Taylor Dome, a small ice dome on the periphery of the East Antarctic Ice Sheet, pass to the north and south of Beacon Valley. Of these, Ferrar Glacier lies to the south and Taylor Glacier to the north. Today, a peripheral lobe of Taylor Glacier extends 1.5 km southward into the mouth of Beacon Valley and terminates in a steep ice cliff up to 25 m high at ~ 1000 m elevation (Fig. 1). A similar lobe occupies the mouth of adjacent Arena Valley. Ablation on these clean, blue-ice lobes is entirely from sublimation and at 1000 m elevation averages 0.18 m water equivalent per year (Robinson, 1984).

Regional Glacial Stratigraphy

Fluctuations of Taylor Glacier are recorded as thin drifts that crop out in lower and central parts of Beacon Valley and adjacent Arena Valley. We recognize two contrasting drift types. One is a mud-rich drift with striated cobbles and granite erratics. The second includes a series of sharp-crested boulder-rich moraines, also with granite erratics, whose map patterns mimic nearby margins of Taylor Glacier (Fig. 1). On the basis of their outcrop patterns and provenance of granite erratics, we infer that both drift types in Beacon and Arena Valleys were deposited from an expanded Taylor Glacier (Marchant et al., 1993a). The best age control for these drifts comes from dated deposits in Arena Valley. There, an age of older than 11.3 Ma for the mud-rich drift comes from $^{40}\text{Ar}/^{39}\text{Ar}$ analyses of volcanic crystals within an overlying ash-avalanche deposit (Marchant et al., 1993a). An age of ca. 2.2 Ma for the oldest boulder-rich moraine comes from ^3He and ^{10}Be exposure ages of boulders atop the farthest up-valley moraine in central Arena Valley (Brook et al., 1993). Morphologically and lithologically similar sharp-crested moraines in lower Beacon Valley are likely of Quaternary and Pliocene age as well, though they remain undated at present.

A key difference in the stratigraphy of lower Beacon and Arena Valleys is that the mud-rich drift on the floor of central Beacon Valley,

the focus of this paper, overlies glacier ice, whereas its correlative drift in Arena Valley rests on weathered sandstone bedrock. In this paper, we follow the usage of Sugden et al. (1995) and refer to the mud-rich drift atop buried glacial ice in central Beacon Valley as Granite drift.

SURFACE STABILITY OF GRANITE DRIFT: THE USE OF COSMOGENIC NUCLIDES

The assertion by Sugden et al. (1995) that pristine and in situ volcanic ashes of Miocene age crop out at the surface of Granite drift seems at odds with the well-developed polygons that characterize the drift surface. To assess the degree of near-surface deformation and convection in Granite drift associated with polygon formation, we measured the abundance of cosmogenic ^3He in two depth profiles that extend from the drift surface down to the buried ice.

Cosmogenic ^3He is one of a group of nuclides produced within rocks at Earth's terrestrial surface by the galactic cosmic-ray flux (Kurz, 1986; Cerling and Craig, 1994). The buildup of these nuclides over time forms the basis of the cosmogenic-nuclide surface-exposure dating technique (Gosse and Phillips, 2001; Clapp et al., 2001). Most previous studies of cosmogenic nuclides in East Antarctica have been applied to defining or testing glacial chronologies (Schäfer et al., 2000a, 2000b; Stone et al., 2000; Tschudi, 2000; Bruno et al., 1997; Ivy-Ochs et al., 1995; Brook et al., 1993, 1995; Brown et al., 1991, 1992) and/or estimating denudation rates (Nishiizumi et al., 1991; Kurz and Brook, 1994; Summerfield et al., 1999). Here, we use the pattern of nuclide concentrations in depth profiles to shed light on the origin and post-depositional history of the deposit (Phillips et al., 1998). In a profile through bedrock, ^3He production by high-energy cosmogenic neutrons follows an exponential trend that systematically decreases with depth (Lal, 1991). Conversely, in a surficial deposit, the pattern of nuclide reduction with depth may display a variety of trends (Phillips et al., 1998). For example, deposits subjected to little burial or surface erosion exhibit profiles with exponentially decreasing concentrations that are identical to the trends seen in bedrock (Fig. 2, profile A). Steady churning of deposits in an active layer by cryological or biological processes produces uniform nuclide concentrations with depth (Fig. 2, profile B). Profiles in tills formed by the progressive concentration of englacial debris during sublimation have downward-decreasing concentrations but are grossly deficient in nuclide concentrations compared to the first trend (Schäfer et al., 2000a; Fig. 2, profile C). Cosmogenic-nuclide depth profiles can also test for the influence of erosion on surface-exposure ages. If clasts on the surface of an otherwise stable deposit are subject to spalling, cracking, or overturning, a distinctive nuclide depth profile with a "dogleg" will result (Fig. 2, profile D). Thus, the internal stability, mode of formation, and degree of surface preservation can all be evaluated with cosmogenic-nuclide depth profiles.

Depth Profiles

We excavated two soil profiles just inward from the margins of two high-centered polygons that cut Granite drift. Each profile exposed a continuous section of Granite drift that was unaffected by active or relict sand-wedge deposits (see subsequent discussion). Profiles 1 and

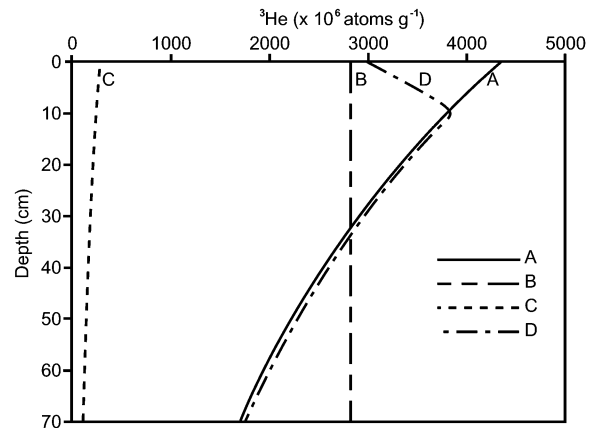


Figure 2. Theoretical cosmogenic ^3He depth profiles. (A) Profile in stable surficial deposit undergoing continuous exposure and zero erosion. (B) Uniform profile in deposit subject to steady mixing by cryoturbation or bioturbation. (C) Profile for sublimation till with sublimation rate of 50 m/m.y. (D) Dogleg profile for stable deposit subjected to surface erosion. The abrupt decrease in near-surface ^3He concentrations results from splitting, spalling, and/or overturning of clasts within 10 cm of the surface. All profiles were computed with $P_0 = 545$ atoms per gram per year; $\rho_{\text{drift}} = 2.0 \text{ g}\cdot\text{cm}^{-3}$; $\Lambda = 150 \text{ g}\cdot\text{cm}^{-2}$; and exposure time = 8 m.y.

2 extended from the ground surface to the top of buried glacier ice, a depth of 70 cm and 38 cm, respectively. Profile 1 was situated 2 m from the margin of an active polygon trough; profile 2 was situated ~ 1 m from the margin of a second, active polygon trough. Cosmogenic ^3He was measured in clinopyroxene contained within individual clasts of Ferrar Dolerite. Amalgamated samples were not used. The depth of each dolerite clast was recorded to ± 1 cm. After the dimensions and bulk densities of each dolerite clast were measured, the samples were crushed and wet-sieved to 60–125 μm . Sized samples were chemically cleaned in an ultrasonic bath with a 1:1 solution of concentrated HCl and distilled water at room temperature. This chemical cleaning removes oxide coatings from mineral grains and facilitates mineral separation but does not affect He concentrations in clinopyroxene (Schäfer et al., 2000a, 2000b). Clinopyroxene (augite and ferro-augite by microprobe analysis) was separated from plagioclase, magnetite, and ilmenite grains by using magnetic and heavy-liquid techniques. Analyzed samples consisted of $>98\%$ clinopyroxene with impurities of plagioclase and ilmenite. Larger grain sizes could not be used because they yielded impure mineral separates with ubiquitous fine-grained intergrowths of pyroxene, ilmenite, and plagioclase.

Mass Spectrometry

He isotopes were measured by using a MAP 215-50 mass spectrometer at the U.S. Geological Survey noble-gas laboratory in Denver, Colorado. Noble gases were extracted from clinopyroxene by heating to 1600 $^{\circ}\text{C}$ for 30–50 min in an all-metal, doubly pumped, electrical-resistance furnace. Step-heating experiments show that all cosmogenic ^3He is released from Ferrar clinopyroxene by 900 $^{\circ}\text{C}$ (Schäfer et al.,

Figure 1. Location map of Beacon Valley, southern Victoria Land.

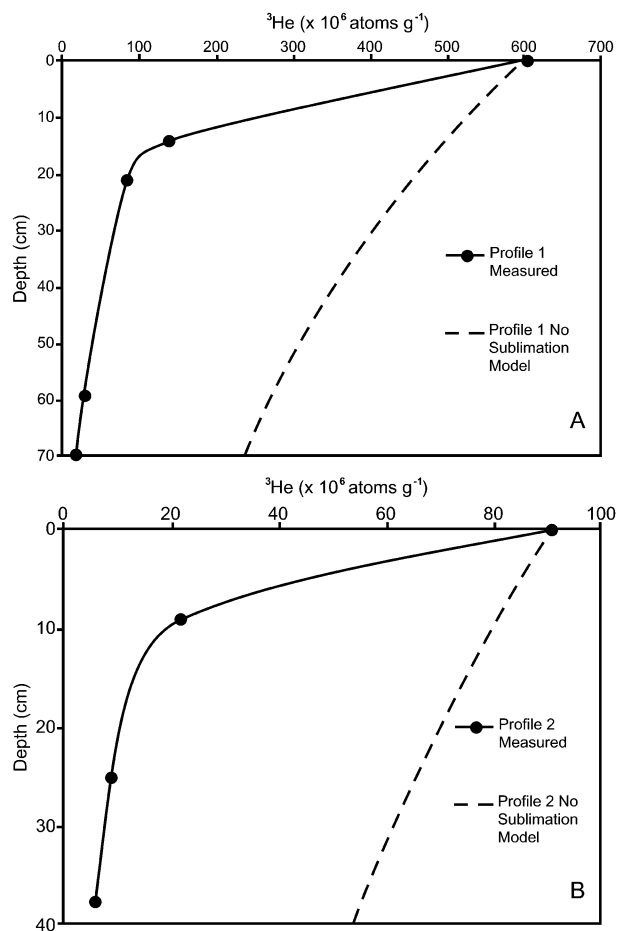


Figure 3. Cosmogenic ³He depth profiles in Granite drift for (A) profile 1 and (B) profile 2. Analytical errors are smaller than the plotting symbols. Dashed lines are nuclide profiles calculated on the basis of surface ³He concentrations and by assuming an exponential decrease in ³He production with depth. Measured concentrations (solid lines) are deficient in ³He, demonstrating that clasts have moved upward from positions of greater shielding as glacier ice sublimated.

2000a, 2000b). Noble gases were purified in an all-metal, gas-extraction line with SAES getters, followed by cryogenic separation of light and heavy noble gases. After cryogenic removal of Ne, He was statically introduced into the mass spectrometer, and He isotopes were analyzed. ⁴He was measured with a Faraday detector, and ³He was measured with a multiplier in ion-counting mode. All He data are corrected for multiplier mass discrimination. Procedural blanks were insignificant (<0.1% of ⁴He) in all samples. Absolute concentrations of ³He and ⁴He were computed from calibrations made by analyzing a 0.0925 ± 0.0005 cm³ aliquot of air with known relative humidity and pressure. Mass spectrometer sensitivity was 1.18 ± 0.05 × 10⁻¹⁹ ³He mol/cps and 6.91 ± 0.18 × 10⁻¹² ⁴He mol/V. Reported analytical errors consist of propagated uncertainties in both counting statistics and sensitivity.

Results

Both profiles exhibit steadily decreasing cosmogenic ³He concentrations (Fig. 3; Table 1). The regularity of the profiles indicates that churning of clasts by cryoturbation has not occurred at these sites despite the formation of patterned ground. Churning that translated clasts vertically and operated over periods of thousands of years would create a uniform nuclide profile pattern or a disrupted exponential trend, depending on the thickness of the active layer. Although exhibiting a steady decrease with depth, subsurface samples in both profiles are deficient in ³He compared with values expected for a continuously exposed stable deposit. This deficiency of ³He in subsurface clasts demonstrates that Granite drift is a lag deposit created by the progressive concentration of englacial debris during the removal of buried ice by sublimation. Clasts have moved upward from positions of greater shielding to their current positions as the ice around them sublimated. The same conclusion was reached by Schäfer et al. (2000a) with surface-exposure dating of a two-point depth profile through Granite drift and by Stone et al. (2000) with ¹⁰Be dating of a three-point depth profile through glacier ice below Granite drift. We address the absolute age of Granite drift after first presenting our model for the formation of its high-centered surface polygons. However, on the basis of the cosmogenic-nuclide data alone, the polygons must form in the absence of widespread churning and sediment reworking.

ORIGIN OF SURFACE POLYGONS

To understand better polygon formation in Beacon Valley, we excavated 63 soil pits (each extending from the ground surface down to

TABLE 1. HELIUM ISOTOPE DATA FROM CLINOPYROXENE IN FERRAR DOLERITE CLASTS

Sample	Depth (cm)	Mass (g)	Thickness (cm)	Density (g/cm ³)	³ He/ ⁴ He (R/R _s)	³ He (10 ⁶ atoms/g)	⁴ He (10 ¹² atoms/g)	Age (Ma)
Depth Profile 1								
ALE-98-8-8	0	0.14532	5.2	3.16	1.89	612 ± 28	234 ± 6	1.18 ± 0.08
ALE-98-8-7	14	0.10832	5.5	2.98	0.22	140 ± 6	463 ± 12	
ALE-98-8-6	21	0.09978	3.6	3.03	0.55	85 ± 4	112 ± 3	
ALE-98-8-3	59	0.14227	4.2	3.26	0.09	28 ± 1	227 ± 1	
ALE-98-8-1	70	0.12148	5.6	3.12	0.06	16 ± 1	206 ± 5	
Depth Profile 2								
ALE-99-01-1	0	0.08066	4.2	2.98	0.14	93 ± 4	487 ± 12	0.18 ± 0.01
ALE-99-01-6	9	0.10279	10.4	2.88	0.05	21 ± 1	298 ± 8	
ALE-99-01-10	25	0.11858	7.3	2.71	0.02	8.9 ± 0.4	351 ± 9	
ALE-99-01-8	38	0.14066	7.0	2.87	0.08	5.4 ± 0.3	53 ± 1	

Notes: All errors are 1σ and include random counting errors, uncertainties in gas calibrations, and for exposure ages, uncertainties in sea-level-high-latitude production rate. Samples were not analyzed in depth order. Exposure ages assume that all ³He is cosmogenic (Schäfer et al., 2000a, 2000b) and that clasts have undergone zero erosion and constant exposure. Ages were computed with altitude scaling that takes in to account Antarctic air-pressure anomalies (Stone, 2000) and a long-term sea-level-high-latitude production rate of 121 ± 6 ³He atoms/g per year (Dunai and Wijbrans, 2000). The local ³He rate is 545 ± 27 atoms/g per year. Corrections to exposure ages for sample thickness were made by assuming exponential attenuation of neutrons with depth, measured bulk densities, and a neutron attenuation coefficient of 150 g·cm⁻². If the altitude scaling of Lal (1991) is used, the exposure ages rise to 1.53 ± 0.10 Ma and 0.21 ± 0.01 Ma.

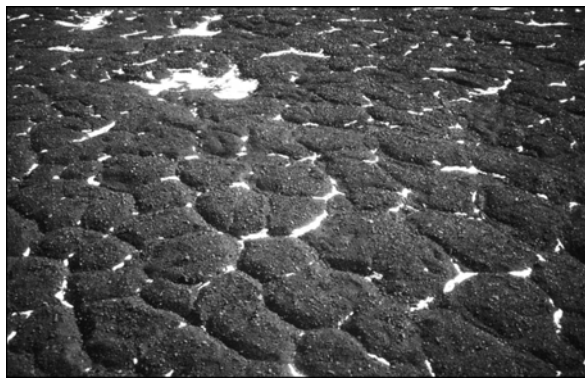


Figure 4. Oblique aerial view of polygons in central Beacon Valley. The average polygon diameter shown in photograph is ~18 m.

TABLE 2. PHYSICAL CHARACTERISTICS OF POLYGONS IN CENTRAL BEACON VALLEY

	Long diameter (m)	Short diameter (m)	Depth of bounding troughs (m)	Width of bounding troughs (m)	Angle of trough walls (°)	Depth to buried glacier ice (cm)
Mean	23	11	1.4	4.7	29	49
<i>N</i> = 19						
Range	35–9	15–6	3.0–1.2	6.4–4.3	34–10	25–80

buried glacier ice and each as much as 12 m long) from 1994 to 1999. At each excavation, we collected multiple samples of gravel (16 mm to 64 mm fraction), sediment (<16 mm fraction), and ash (observed in wedges and subhorizontal lenses, e.g., Marchant et al., 1996; Sugden et al., 1995). In addition, we retrieved samples of the underlying glacier ice (either from shallow cores <2.0 m deep or blocks 30 cm³ in size) and superposed secondary-ice lenses.

Morphology

High-centered polygons at the surface of Granite drift are roughly hexagonal in plan view and range in diameter from 10 to 35 m (Fig. 4; Table 2; Ugolini et al., 1971). V-shaped troughs that separate adjacent polygons are as much as 3 m deep. Boulders and cobbles commonly rest at the floor of these troughs. Roughly 5% of the troughs reveal steps that mark recent slumping, the slip-surface of which is noticeably less weathered than adjacent regions. Commonly, wind-blown snow is trapped in deep parts of most polygon troughs (Fig. 4). The central part of each polygon is generally level, though it ends abruptly in steep slopes (angled from 25°–30°) that lead downward to the base of marginal troughs.

Internal Stratigraphy

Granite drift is loose, unconsolidated, and <1.0 m thick. It rests with sharp, planar contacts on the surface of buried glacier ice. It exhibits a seasonally moist surface-weathering layer that from top to bottom includes (1) a cobble-and-boulder cap with patches of weathered and fragmented dolerite and sandstone gravel and (2) a subsurface horizon of medium- to coarse-grained, iron oxide-coated quartz grains and dolerite grus down to a depth of ~10–15 cm. Below this surface-

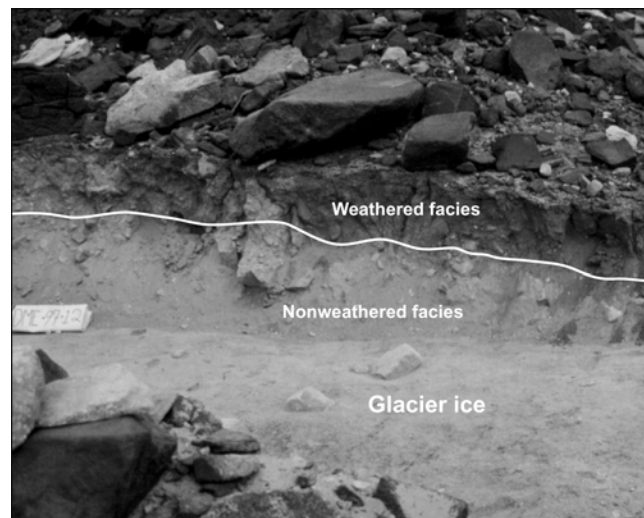


Figure 5. Unweathered Granite drift exposed above buried glacier ice in soil pit DME-97-12. White placard (labeled DME 97-12) at center left is ~35 cm long.

weathering layer, Granite drift is perennially dry and reveals interbedded lenses and wedges of weathered and nonweathered facies.

Nonweathered Facies

The nonweathered facies of Granite drift is poorly sorted and matrix supported. It mantles glacial ice at polygon centers (Fig. 5; Table 3). Its silty matrix is composed largely of quartz grains derived from Beacon Supergroup rocks. Erratics of granite and aplite constitute from 1% to 5% of the gravel fraction. On average, 25% of the sampled clasts between 16 mm and 64 mm show glacial striations and/or polish and molding. This facies of Granite drift is similar in texture, weathering state, color (7.5 YR 8/2–10 YR 7/3, light gray to buff), and mineral assemblage to debris bands within the underlying glacier ice (Table 3).

Weathered and Winnowed Facies

The weathered and winnowed facies of Granite drift is coarse grained and clast supported (Table 3); 90% of the gravel- and cobble-sized clasts within this facies exhibit desert varnish and/or wind-faceted edges. Overall, the facies is reddish brown (5 YR 4/3) to brown (10YR 5/4) in color. Quartz grains and weathered dolerite grus, which together comprise the sandy matrix, are covered with thin iron oxide coatings.

The weathered and winnowed facies of Granite drift occurs in three stratigraphic settings: (1) as the oxidized near-surface horizon previously described; (2) as near-horizontal subsurface lenses from 2 cm to ~30 cm thick that feature sharp stratigraphic contacts with unweathered drift; and (3) as downward-pointing, V-shaped wedges that lie directly beneath troughs delineating surface polygons.

Volcanic Ash

Minimally disturbed air-fall volcanic-ash deposits occur in Granite drift. These ash deposits are almost always associated with the weathered and winnowed facies of Granite drift. Stratigraphic contacts with nonvolcanic sediments are sharp, and ash is not disseminated throughout Granite drift.

For each ash deposit examined, its purity, uniform geochemistry,

TABLE 3. TEXTURAL CHARACTERISTICS OF GRANITE DRIFT AND SEDIMENT FROM UNDERLYING GLACIER ICE

Unit	Permeability (cm/s)	Texture (matrix < 1.6 cm)			Abundance of erratic clasts (%)	Abundance of glacially molded or striated clasts	Weathering characteristics	Internal stratigraphy	Stratigraphic contacts	Sediment in ice (%)
		Gravel (%)	Sand (%)	Mud (%)						
Granite drift <i>N</i> = 14	2.3014×10^{-4}	26	56	18	5	23%	Matrix unstained	Nonstratified and poorly sorted. Rests directly on buried glacier ice with smooth planar contacts.	Sharp, dry contact with underlying ice. White clay-rich film <0.2 mm) coats top of ice surface	N.A.
Sediment from buried glacier ice <i>N</i> = 9	N.A.	27	56	17	4	36%	Matrix unstained	Debris bands from 5 to 15 cm thick; alternate with layers of clear ice. Foliation generally trends east-west	Foliation in ice generally trends east-west, and is unaffected by contraction cracks	3.1 sediment by volume (neglecting air bubbles); 8.5% sediment by weight
Sand-wedge deposits <i>N</i> = 8	4.2402×10^{-2}	7	83	10	3	N.D.	Matrix sands are heavily stained	Well-sorted, vertically stratified to massive sands and gravels	Sharp contacts, crosscuts buried ice and Granite drift	N.A.

Note: N.A.—not applicable. N.D.—not determined because desert varnish obscures striations if present.

sharp stratigraphic contacts with adjacent deposits, and preservation of delicate features on glass shards all point to an origin by direct air fall onto the surface of Granite drift (e.g., Sugden et al., 1995; Marchant et al., 1996). A likely scenario is that during eruptions of nearby McMurdo Group volcanic centers (100 km to 150 km distant, Kyle, 1990; Marchant et al., 1996), ash-fall ash was trapped in deep polygon troughs, just as modern snowfall is trapped there today. In cross section, many ash-fall deposits are wedge-shaped, reflecting the initial geometry of polygon troughs (e.g., Marchant et al., 1996) (Fig. 6). These wedge-shaped ash deposits are generally nested within larger, V-shaped wedges of weathered and winnowed Granite drift. In places, ash deposits may occur as thin stringers of volcanic ash between conformable layers of weathered Granite drift. These stringers likely form as ash within overlying wedge-shaped deposits percolates downward into narrow cracks (see subsequent discussion). In rare instances where ash layers <1.0 cm thick occur sandwiched between nonweathered drift, we infer that the ash percolated down contraction cracks to a depth below that possible for sandy, weathered, and winnowed Granite drift. We note that volcanic ash is not found within buried glacier ice.

Buried Glacier Ice

The surface of the buried glacier ice beneath Granite drift mimics the modern ground topography. The ice surface is nearly horizontal beneath polygon centers and dips sharply toward polygon troughs. The ice-surface slope beneath polygon troughs equals or exceeds the ground slope above. Such characteristics suggest that the surface slope of the buried glacier ice drives the modern ground topography.

A network of thermal-contraction cracks (i.e., cracks resulting from seasonal cooling and contraction of near-surface ice) cuts the buried glacier ice (e.g., Lachenbruch, 1961, 1962). When open, contraction cracks may receive sediment through downward percolation of weathered Granite drift (e.g., Berg and Black, 1966; Black, 1973). Successive crack-and-fill episodes create a wedge-shaped, downward-tapering deposit of weathered Granite drift that borders active contraction cracks. These deposits are vertically stratified and display a coarsening-upward stratigraphy that reflects the progressive taper in width of thermal-con-



Figure 6. South face of soil pit DME-98-15 showing a well-preserved ash wedge (light colored) above buried glacier ice in central Beacon Valley. Ash lies at the center of an inactive sand-wedge deposit composed of weathered and winnowed Granite drift.

traction cracks with depth (e.g., Ugolini et al., 1971). These deposits are equivalent to the tessellations or sand wedges of Péwé (1959). These sand-and-gravel wedges are as much as 30 cm wide at the top and at least 2 m deep (wedges extended beyond the depth of field excavations). We observed open cracks (from 1 to 2 cm in thickness) at the center of each sand wedge excavated during the months of November to January, 1995–1998, but we have no data as to whether the cracks were open at other times.

As reported in Sugden et al. (1995), the buried glacier ice consists of equigranular 10 mm crystals along with dispersed rock debris and numerous debris bands from 5 to 15 cm thick. Enveloping the debris bands are layers of clear ice and white, bubbly foliated ice. Oxygen isotope analyses of the buried glacier ice yield $\delta^{18}\text{O}$ values with a mean value of -33.2‰ (seven samples with a range of -33.0‰ to -33.6‰ ; Sugden et al., 1995). All analyses are aligned in a δD versus $\delta^{18}\text{O}$ diagram on a precipitation slope of ~ 8 (Sugden et al., 1995). Although significant melting and refreezing of a water body produces a freezing slope lower than 8, minute amounts of melting followed by refreezing will still be aligned on the precipitation slope (Souchez and Jouzel, 1984). The layers of clear and white, bubbly foliated ice that fall on a precipitation slope of ~ 8 indicate that the buried glacier ice has undergone minor basal regelation at the pressure melting point (Iverson and Souchez, 1996) and has subsequently refrozen with no further phase changes.

Ice-fabric analyses reported in Sugden et al. (1995) show that the direction of ice flow was up-valley and oblique to the longitudinal axis of Beacon Valley. The strike of the foliation, as recorded by an obvious alignment of clasts and debris bands within the buried glacier ice, is generally due east across the valley axis. This foliation consistently passes across contraction cracks without deformation. Such a relationship shows that (1) foliation in the ice is not caused by progressive growth of ice wedges in polygon troughs and (2) sand-wedge growth has not induced lateral flow within adjacent glacier ice (e.g., Murton et al., 2000).

Secondary-Ice Lenses

Our soil excavations show that secondary ice cements together iron oxide-stained quartz grains and weathered dolerite grus at the base of polygon troughs. The ice occupies pores in the weathered and winnowed facies of Granite drift and forms a 2–3-cm-thick, ice-cemented, sandy layer that rests directly on buried glacier ice. Stable isotope data from this ice show it to be derived from the melting and refreezing of snow enriched in heavy isotopes by evaporative processes. On a δD versus $\delta^{18}\text{O}$ plot, the ice that cements the quartz grains and dolerite grus is aligned along a slope of ~ 5 , considerably lower than that for the buried glacier ice and modern snow, both of which fall on a precipitation slope of ~ 8 (Fig. 7). The intersection point between the precipitation slope and the line on which the ice that cements the sand grains is aligned is very close to modern snow samples, suggesting derivation of the secondary ice from snow. The deuterium excesses ($d = \delta\text{D} - 8\delta^{18}\text{O}$) of ice in the ice-cemented sand samples (-85‰ to -46‰) are much more negative than in modern snow samples (-4‰ to $+2\text{‰}$). This effect is best explained by a highly evaporated source for the ice in the cemented samples. Although the deuterium excess of ice can be lowered by melting followed by partial refreezing, the change in deuterium excess never exceeds a few per mil. Conversely, evaporation of snow also produces a shift off of the precipitation slope but with a large decrease in the deuterium excess (Jouzel and Merlivat, 1984; Craig, 1961). The simplest scenario in accord with the isotopic data is that snow accumulated in polygon troughs, underwent significant evaporative loss and partial summer melting, and percolated into permeable sand layers where refreezing above the buried glacier ice occurred. Downward percolation of meltwater is likely facilitated by the depression of the freezing point by the high salt content of Dry Valleys soils (Claridge and Campbell, 1977; Bockheim, 1990). We have observed small amounts of snowmelt in polygon troughs adjacent

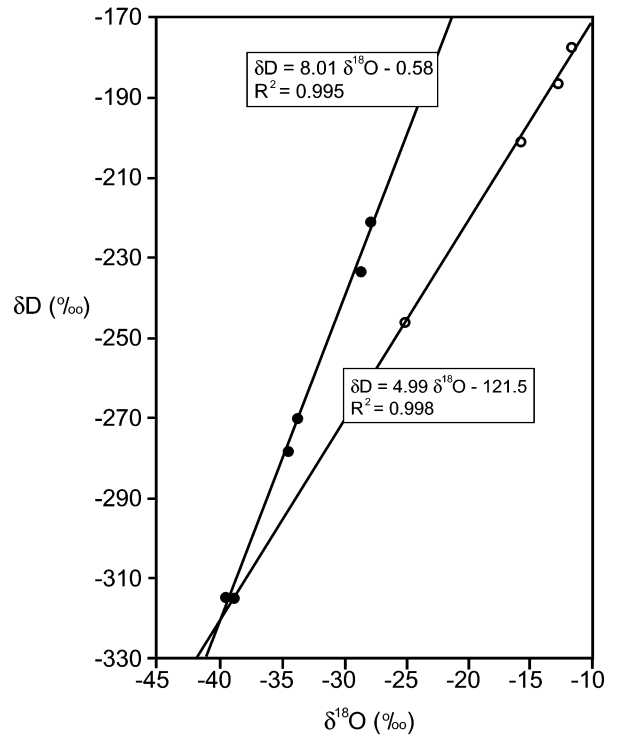


Figure 7. Plot of δD vs. $\delta^{18}\text{O}$ for modern snow in Beacon Valley and ice in ice-cemented sand-grain lenses at the base of polygon troughs. Solid circles show values for modern snowfall; open circles record values for ice in ice-cemented sand grains. The accuracy of the measurements is 0.5‰ for δD and 0.05‰ for $\delta^{18}\text{O}$. Analyses were performed at the Centre d'Études Nucléaires de Saclay, France. See text for explanation.

to dark dolerite clasts on sunny summer days when radiative heating was sufficient to overcome subzero air and ground temperatures.

Model for Polygon Development in Beacon Valley

The high-centered, surface polygons and complex internal stratigraphy of Granite drift likely result from coeval sublimation and thermal contraction of debris-rich glacier ice. Simple ice sublimation—without thermal contraction—would only produce a poorly sorted lag deposit of unweathered sublimation till topped by an oxidized surface-weathering horizon (Fig. 8A; Shaw, 1976, 1988). However, when combined with thermal contraction of the underlying glacier ice, the two processes can produce the observed stratigraphy and surface morphology of Granite drift and are fully consistent with the cosmogenic-nuclide data for surface stability outside polygon troughs and the presence of in situ ashes of Miocene age (Sugden et al., 1995) at the drift surface.

The weathered and winnowed facies of Granite drift at polygon troughs originates as loose grains from the surface percolate downward into open contraction cracks (Figs. 8B and 9A). Downward percolation through narrow cracks ($\sim 1\text{--}2$ cm wide) produces a coarse and highly porous gravel-and-cobble lag that lines the base of polygon troughs. The lag represents material too large to pass into contraction cracks (Figs. 8C and 9B). Because the permeability of this lag deposit is at least two orders of magnitude higher than that of unweathered Granite

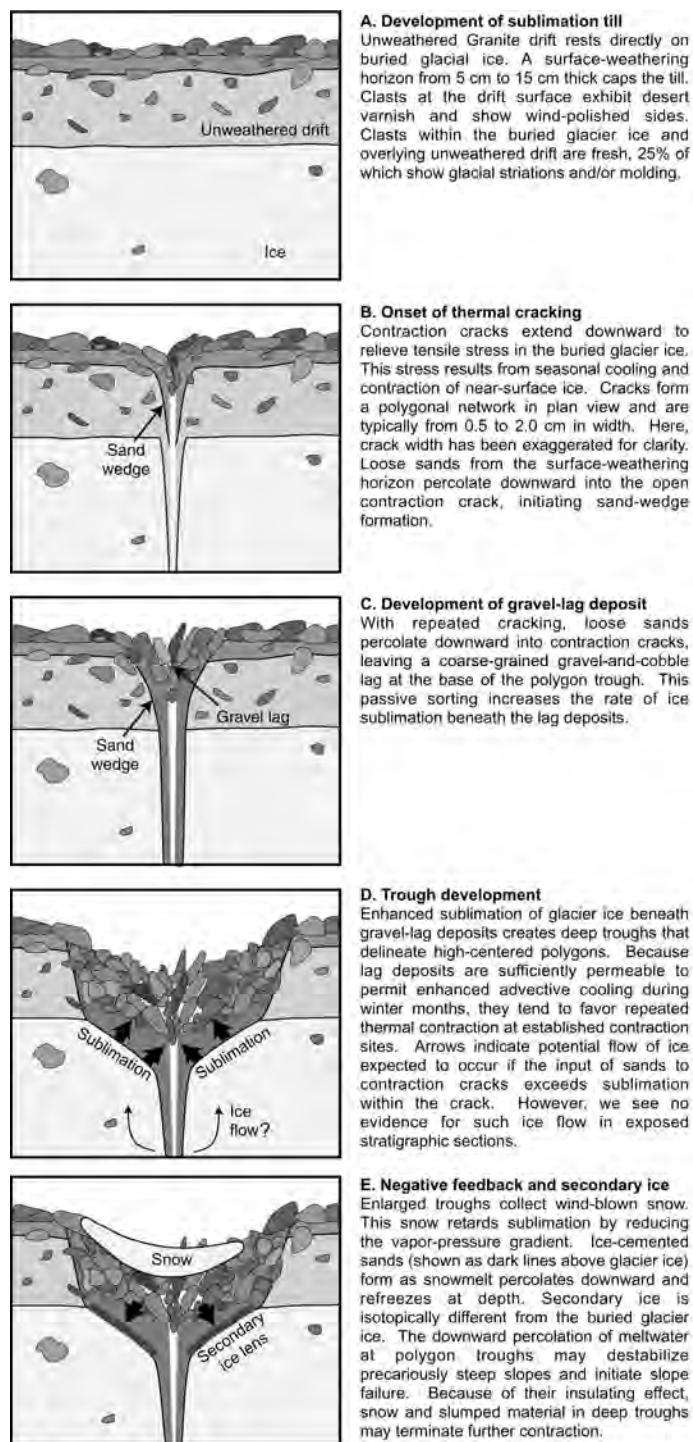


Figure 8. Sequential sketches show the key stages in the formation of high-centered polygons over buried glacier ice in central Beacon Valley.

drift at polygon centers (Table 3), ice sublimation below polygon troughs is enhanced relative to that below unweathered drift of low permeability at polygon centers. A consequence of enhanced ice sublimation at sites of active thermal contraction is the development of

large, funnel-shaped troughs that delineate surface polygons in plan view (Figs. 8D and 9B). These troughs form as the underlying ice surface lowers and produce the great relief of high-centered polygons of Beacon Valley. A last but important point is that because lag deposits above active contraction cracks are sufficiently permeable to permit enhanced advective cooling during winter months, they tend to favor repeated thermal contraction at established contraction sites (e.g., Pissart, 1990).

Once polygon troughs are deepened to the extent that they become preferred sites for deposition of windblown snow, a negative feedback operates that tends to shut down sublimation in troughs and, possibly, to initiate a shift in the loci of thermal contraction (Fig. 8E). As previously discussed, the most likely origin for ice-cemented grains at the base of polygon troughs is the melting of snow (coupled with strong sublimation), downward percolation, and subsequent refreezing at depth (downward movement of liquid water may be related to elevated salt concentrations of Dry Valley soils, McKay et al., 1998). This downward transfer and refreezing of liquid water (and most likely vapor as well) seals the underlying glacier ice (Fig. 9C). Further sublimation of the buried glacier cannot proceed until all of the overlying secondary ice first sublimates (see also Hindmarsh et al., 1998). The downward percolation of meltwater along polygon troughs likely destabilizes precariously steep slopes at trough walls and leads to slump failure (the resulting scarps are readily apparent in the field). These processes tend to shut down "enhanced" sublimation at polygon troughs and may, owing to the insulating effect of slumped debris and snow, lead to a shift in the loci of thermal contraction (e.g., Goodrich, 1982; Mackay, 1993; Law and van Dijk, 1994).

A shift in the loci of thermal contraction, coupled with continued slow sublimation of glacier ice, yields the subhorizontal layers of weathered and winnowed Granite drift commonly seen in stratigraphic section. These tilted layers are, in effect, abandoned sand-wedge deposits tilted to one side. Air-fall volcanic-ash deposits, commonly associated with these tilted sand wedges, were deposited in cracks and furrows when the wedges were upright and active (Marchant et al., 1996; Sugden et al., 1995). The absence of upturned debris bands or deflected foliation in glacier ice adjacent to active sand wedges (e.g., Mackay, 1980; Murton et al., 2000) suggests that the wedges are starved of sediment. Figure 10 shows our model for the evolution of Granite drift and surface polygons in Beacon Valley. This model likely applies to other drifts in the Dry Valleys region that, long ago, may have formed atop stagnant glacial ice in a manner similar to that of Granite drift (e.g., Marchant et al., 1993a, 1993b, 1994; Bockheim, 1995).

AGE CONTROL

Three conclusions arise from our morphologic, sedimentologic, and cosmogenic-nuclide analyses of Granite drift in Beacon Valley. The first is that Granite drift is generally stable at polygon centers; only polygon troughs are active. The second is that the surface morphology of Granite drift is tied to sublimation of the underlying glacier ice; the rate of sublimation is influenced by the development of porous gravel-and-cobble-lag deposits that form above thermal-contraction cracks. The third is that ash falls within abandoned sand-wedge deposits are reliable chronostratigraphic markers that provide minimum ages for Granite drift and underlying glacier ice; this is true because wedge-shaped ash-fall deposits have not been reworked by patterned-ground formation. The oldest dated in situ ash-fall deposit within Granite drift is 8.1 Ma (Sugden et al., 1995). The fact that some regions of Granite drift have escaped

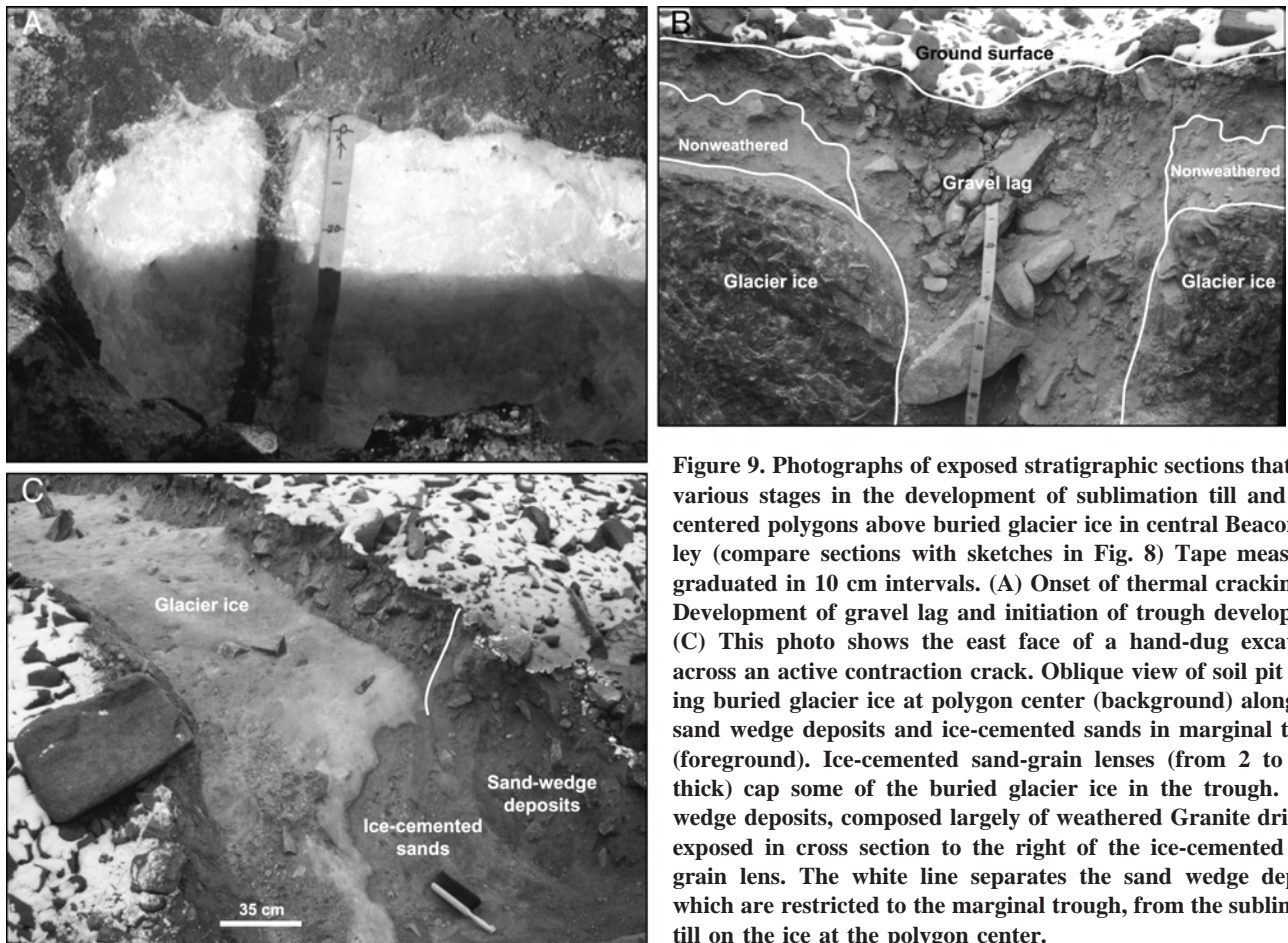


Figure 9. Photographs of exposed stratigraphic sections that show various stages in the development of sublimation till and high-centered polygons above buried glacier ice in central Beacon Valley (compare sections with sketches in Fig. 8) Tape measure is graduated in 10 cm intervals. (A) Onset of thermal cracking. (B) Development of gravel lag and initiation of trough development. (C) This photo shows the east face of a hand-dug excavation across an active contraction crack. Oblique view of soil pit showing buried glacier ice at polygon center (background) along with sand wedge deposits and ice-cemented sands in marginal trough (foreground). Ice-cemented sand-grain lenses (from 2 to 5 cm thick) cap some of the buried glacier ice in the trough. Sand-wedge deposits, composed largely of weathered Granite drift, are exposed in cross section to the right of the ice-cemented sand-grain lens. The white line separates the sand wedge deposits, which are restricted to the marginal trough, from the sublimation till on the ice at the polygon center.

modification by patterned ground for at least 8.1 Ma indicates long-term geomorphic stability of individual polygons. Once established, polygon troughs likely persist for as long as 10^5 – 10^6 yr.

If our model for polygon development is correct, then exposure ages at the drift surface should be youngest at polygon margins, where intermittent slumping periodically refreshes the drift surface on time scales of 10^4 – 10^5 yr. Our measured ages for Granite drift based on cosmogenic ^3He abundance in surface clasts at the top of two sampled profiles just inward from active polygon margins are 1.18 ± 0.08 Ma (profile 1) and 0.18 ± 0.01 (profile 2) (Table 1). Like other cosmogenic-nuclide exposure ages from Granite drift (Schäfer et al., 2000a; Tschudi, 2000), these ages assume zero erosion of the surface and vary by an order of magnitude over short distances. Though erosion clearly occurs at the surface of Granite drift (as indicated by split cobbles and widespread dolerite grus, Schäfer et al., 2000a; Lewis, 2000), the difference in our exposure ages, as well as their overall young age, cannot be explained by surface weathering alone, for the following reasons: (1) There is no evidence for the “dogleg” profile pattern that would arise from spalling, cracking, or overturning of clasts on an otherwise stable deposit. (2) If the exposure age at the top of profile 2 was due to local clast erosion, with the rest of the profile having had an exposure time equivalent to or greater than that of profile 1 (1.18 Ma), then the total ^3He inventory would be at least an order of magnitude greater. (3) If the Granite drift at the two locations sampled had been

subject to continuous exposure and steady sublimation for >8.1 m.y., then subsurface concentrations in both profiles would be several orders of magnitude greater than observed. Thus, though our cosmogenic-nuclide data are consistent with stable polygon centers, they indicate that Granite drift is likely renewed at the margins of polygon troughs. Our cosmogenic ^3He surface-exposure ages of 1.18 Ma and 0.18 Ma likely reflect the elapsed time since slumping along trough walls. The long intervals between slump events (at least 1.18 Ma for profile 1) at polygon margins (the most dynamic part of Granite drift) are fully consistent with the assertion that parts of Granite drift, and hence its underlying glacier ice, are older than 8.1 Ma. We emphasize here that Granite drift is not everywhere older than 8.1 Ma, but rather that only parts of the drift sheet are at least that old. Some Granite drift is forming today, notably where modern ice sublimation adds new sediment to the base of this evolving, though ancient, drift sheet.

Sublimation rates estimated by using the method of Schäfer et al. (2000a) are 20 m/m.y. and 90 m/m.y. for profiles 1 and 2, respectively. These rates are maximum end-member rates for Granite drift sublimation for the following reasons: (1) They are calculated by assuming constant and steady sublimation. Our stratigraphic evidence suggests that rates of sublimation vary both spatially and temporally, being highest at polygon troughs and lowest at polygon centers. The relatively young and variable exposure ages for our profiles indicate that they are near enough to troughs to have been affected by slumping.

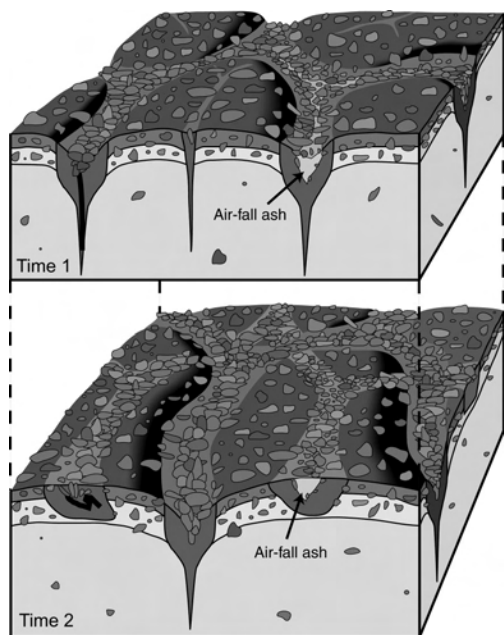


Figure 10. Conceptual model for the evolution of Granite drift and high-centered polygons over buried glacier ice in Beacon Valley. The block diagrams trace the sequence of patterned-ground formation through time. Deep polygon troughs with well-developed sand-wedge deposits shown in the upper block diagram become relict, or abandoned, troughs in the lower block diagram. In contrast, developing troughs in the upper block diagram are well established with mature sand-wedge deposits in the lower block diagram. This pattern of thermal contraction and trough development, in conjunction with continued ice sublimation, explains the areal and stratigraphic distribution of weathered and nonweathered Granite drift in central Beacon Valley. It is consistent with our cosmogenic ^3He isotope data that call for stable surfaces inward from polygon troughs. Ash deposits in the upper block diagram are shown as (1) a thin black, vertical line at the center of an active sand wedge showing where air-fall ash fell into an open contraction crack and (2) a light-colored, wedge-shaped deposit showing where air-fall ash was trapped in a deep polygon trough (later covered with debris slumped from trough walls). The lower block diagram shows expected changes in the configuration of these ash deposits at some distant time.

Following slumping, sublimation rates decrease rapidly as new low-permeability till is added to the ice surface. (2) Calculated rates are tied to surface-exposure ages that assume zero clast erosion and are therefore minimum estimates, making our apparent sublimation rates clear overestimates. Our maximum sublimation estimates bracket rates of ~ 5 m/m.y. found by Schäfer et al. (2000a) and 50 m/m.y. estimated by Stone et al. (2000) using independent methods and are orders of magnitude lower than those computed on theoretical grounds by Hindmarsh et al. (1998). Collectively, the rates suggest that glacial ice beneath Granite drift can survive for millions of years.

WIDER IMPLICATIONS

Although most models for the development of high-centered polygons incorporate convective flow in near-surface active layers, we show

here that polygons in Beacon Valley form without lateral flow at polygon centers. The only active regions of Granite drift are those that lie above and immediately adjacent to thermal-contraction cracks. Because the polygons of central Beacon Valley are likely close analogues for similar features on Mars (Anderson et al., 1972), we argue that some of the rough hexagons of Utopia Planitia (Hiesinger and Head, 2000) may have formed in a manner similar to those of Beacon Valley, where liquid water is sparse and traditional active layers are rare to nonexistent. Our model of accentuated trough development from enhanced sublimation beneath cobble lags at the base of polygon troughs may help explain the great width of some of the polygon troughs on Mars (e.g., Pechmann, 1980).

CONCLUSIONS

Measured concentrations of in situ-produced cosmogenic ^3He in two profiles through Granite drift show a steady decrease with depth, indicating negligible mixing of clasts by cryoturbation despite patterned-ground formation. Significant churning or convection of Granite drift—as would occur if the underlying ice had thawed to produce a seasonal active layer—has not occurred at least since 1.18 Ma and most likely has not occurred since 8.1 Ma.

Subsurface dolerite clasts are grossly deficient in cosmogenic ^3He compared with expected values for a stable deposit extrapolated from surface concentrations. This deficiency in ^3He is strong evidence that Granite drift is a lag deposit created by progressive sublimation of underlying glacier ice. Clasts have moved upward from positions of greater cosmogenic-nuclide shielding to their current positions as the overlying ice sublimed.

The combination of thermal contraction and sublimation of buried glacier ice in Beacon Valley leads to abrupt temporal and spatial variations in the texture of Granite drift. These textural variations influence the rate and location of sublimation of the remaining glacier ice, which in turn influences polygon morphology.

Polygon troughs form above sites of active thermal contraction, where high-porosity and high-permeability cobble-and-gravel lag deposits permit greater ice sublimation than beneath unweathered, mud-rich drift at polygon centers. Once polygon troughs deepen sufficiently, they trap windblown snow and initiate a negative feedback that slows further sublimation of the underlying glacier ice. This negative feedback involves the development of secondary-ice lenses at the base of polygon troughs. $\delta^{18}\text{O}$ and δD analyses of the ice that cements the sand grains to form a secondary-ice lens indicate an origin from snowmelt (coupled with strong sublimation) and subsequent refreezing at depth. The isotopic composition of the secondary ice that cements the sand grains is significantly different from that of the buried glacier ice below.

Downward percolation of meltwater at polygon troughs may help destabilize precariously steep slopes at trough walls and initiate slope failure (the scarps of which are readily apparent in the field). Such slumping, through removal of thick layers of drift, explains relatively young and variable cosmogenic ^3He surface-exposure ages of 1.18 Ma and 0.18 Ma near active polygon margins. Overall, the snow cover at polygon troughs, the buried secondary-ice lenses at depth, and the slumps that tend to fill polygon troughs may, owing to their insulating effects, lead to a shift in the loci of thermal contraction.

A shift in the loci of thermal contraction, coupled with continued slow sublimation of glacier ice, yields subhorizontal layers of weathered Granite drift that are abandoned sand-wedge deposits tilted to one

side. This process explains why unweathered Granite drift and weathered Granite drift are interbedded in near-horizontal layers above buried glacier ice. Air-fall volcanic-ash deposits, commonly associated with these tilted sand wedges, were deposited in cracks and furrows when the wedges were upright and active (Marchant et al., 1996; Sugden et al., 1995).

Lastly, the cosmogenic-isotope data, along with the evidence for air-fall ash deposits of Miocene age, indicate that Granite drift has not developed a saturated active layer over the past 1.18 m.y. to 8.1 m.y., even though buried glacial ice lies from 25 to 80 cm below the ground surface. We suggest that similar-sized polygons on Mars that occur over buried ice in Utopia Planitia may have formed in a manner similar to those of Beacon Valley, where liquid water is sparse and traditional active layers are likely rare to nonexistent.

ACKNOWLEDGMENTS

This work was funded and supported by the Division of Polar Programs of the U.S. National Science Foundation. We thank J. Jouzel for hydrogen and oxygen isotope analyses of the ice and snow samples completed at the Centre d'Études Nucléaires de Saclay, France. We also thank D.H. Clark, P.R. Bierman, S. Lundstrom, and C.A. Johnson for helpful reviews. Cosmogenic ^3He measurements were supported by grant R34924 from the National Environmental Research Council, United Kingdom, and by the Branch of Isotope Geology, U.S. Geological Survey. We thank J.K. Willenbring and K. Tonka for excellent assistance in the field, as well as the staff at the Berg Field Center and pilots with VXE-6 and PHI. L.M. Mills-Herring assisted with mass spectrometry.

REFERENCES CITED

- Anderson, D.M., Gatto, L., and Ugolini, F.C., 1972, An Antarctic analog of Martian permafrost terrain: *Antarctic Journal of the United States*, v. 7, no. 4, p. 114–115.
- Barrett, P.J., 1981, History of the Ross Sea region during the deposition of the Beacon Supergroup 400–180 million years ago: *Journal of the Royal Society of New Zealand*, v. 11, p. 447–458.
- Berg, T.E., and Black, R.F., 1966, Preliminary measurements of growth of nonsorted polygons, Victoria Land, Antarctica, in Tedrow, J.F.C., ed., *Antarctic soils and soil forming processes*: American Geophysical Union Antarctic Research Series, v. 8, p. 61–108.
- Black, R.F., 1973, Growth of patterned ground in Victoria Land, Antarctica, in *Permafrost Second International Conference*: Washington, D.C., National Academy of Sciences, p. 193–203.
- Bockheim, J.G., 1990, Soil development rates in the Transantarctic Mountains: *Geoderma*, v. 47, p. 59–77.
- Bockheim, J.G., 1995, Permafrost distribution in the southern circumpolar region and its relation to the environment: A review and recommendation for further research: *Permafrost and Periglacial Processes*, v. 6, p. 27–45.
- Brook, E.J., Kurz, M.D., Ackert, R.P., Jr., Denton, G.H., Brown, E.T., Raisbeck, G.M., and Yiu, F., 1993, Chronology of Taylor Glacier advances in Arena Valley, Antarctica, using in situ cosmogenic ^3He and ^{10}Be : *Quaternary Research*, v. 39, p. 1–10.
- Brook, E.J., Kurz, M.D., Ackert, R.P., Raisbeck, G., and Yiu, F., 1995, Cosmogenic nuclide exposure ages and glacial history of late Quaternary Ross Sea drift in McMurdo Sound, Antarctica: *Earth and Planetary Science Letters*, v. 131, p. 41–56.
- Brown, E.T., Edmond, J.M., Raisbeck, G.M., Yiu, F., Kurz, M.D., and Brook, E.J., 1991, Examination of surface exposure ages of Antarctic moraines using in situ produced ^{10}Be and ^{26}Al : *Geochimica et Cosmochimica Acta*, v. 55, p. 2269–2283.
- Brown, E.T., Brook, E.J., Raisbeck, G.M., Yiu, F., and Kurz, M.D., 1992, Effective attenuation lengths of cosmic producing Be-10 and Al-26 in quartz: Implications for exposure age dating: *Geophysical Research Letters*, v. 19, p. 369–372.
- Bruno, L.A., Baur, H., Graf, T., Schluchter, C., Signer, P., and Wieler, R., 1997, Dating of Sirius Group tillites in the Antarctic Dry Valleys with cosmogenic ^3He and ^{21}Ne : *Earth and Planetary Science Letters*, v. 147, p. 37–54.
- Cerling, T.E., and Craig, H., 1994, Geomorphology and in situ cosmogenic isotopes: *Annual Reviews of Earth and Planetary Sciences*, v. 22, p. 273–317.
- Clapp, E.M., Bierman, P.R., Nichols, K.K., Pavich, P., and Caffee, M., 2001, Rates of sediment supply to arroyos from upland erosion determined using in situ produced cosmogenic ^{10}Be and ^{26}Al : *Quaternary Research*, v. 55, p. 235–245.
- Claridge, G.G.C., and Campbell, I.B., 1977, The salts in Antarctic soils, their distribution and relationship to soil processes: *Soil Science*, v. 28, p. 377–384.
- Craig, H., 1961, Isotopic variations in meteoric waters: *Science*, v. 133, p. 1702–1703.
- Denton, G.H., and Marchant, D.R., 2000, The geologic basis for a reconstruction of a grounded ice sheet in McMurdo Sound, Antarctica, at the Last Glacial Maximum: *Geografiska Annaler*, v. 82A, p. 167–211.
- Denton, G.H., Armstrong, R.L., and Stuiver, M., 1971, The late Cenozoic glacial history of Antarctica, in Turekian, K.K., ed., *The late Cenozoic glacial ages*: New Haven, Connecticut, Yale University Press, p. 267–306.
- Denton, G.H., Bockheim, J.G., Wilson, S.C., and Stuiver, M., 1989, Late Wisconsin and early Holocene glacial history of the inner Ross Embayment, Antarctica: *Quaternary Research*, v. 31, p. 151–182.
- Denton, G.H., Sugden, D.E., Marchant, D.R., Hall, B.L., and Wilch, T.I., 1993, East Antarctic Ice Sheet sensitivity to Pliocene climatic change from a Dry Valleys perspective: *Geografiska Annaler*, v. 75A, p. 155–204.
- Dunai, T.J., and Wijbrans, J.R., 2000, Long-term cosmogenic He-3 production rates (152 ka–1.35 Ma) from Ar-40/Ar-39 dated basalt flows at 29 degrees N latitude: *Earth and Planetary Science Letters*, v. 176, p. 147–156.
- Goodrich, L.E., 1982, The influence of snow cover on the ground thermal regime: *Canadian Geotechnical Journal*, v. 19, p. 414–432.
- Gosse, J.C., and Phillips, F.M., 2001, Terrestrial in situ cosmogenic nuclides: Theory and application: *Quaternary Science Reviews*, v. 20, p. 1475–1560.
- Hallet, B., and Prestrud, S., 1986, Dynamics of periglacial sorted circles in western Spitsbergen: *Quaternary Research*, v. 26, p. 81–99.
- Hallet, B., and Waddington, D.E., 1991, Buoyancy forces induced by freeze-thaw in the active layer: Implications for diapirism and soil circulation, in Dixon, J.C., and Abrahams, A.D., eds., *Periglacial geomorphology*: West Sussex, UK, John Wiley and Sons, p. 251–279.
- Hiesinger, H., and Head, J.W., III, 2000, Characteristics and origin of polygonal terrain in southern Utopia Planitia, Mars: Results from Mars Orbiter laser altimeter and Mars Orbiter camera data: *Journal of Geophysical Research*, v. 105E, p. 11999–12022.
- Hindmarsh, R.C.A., van der Wateren, F.M., and Verbers, A.L.L.M., 1998, Sublimation of ice through sediment in Beacon Valley, Antarctica: *Geografiska Annaler*, v. 80A, p. 209–219.
- Iverson, N.R., and Souchez, R.A., 1996, Isotopic signature of debris-rich ice formed by regelation into a subglacial sediment bed: *Geophysical Research Letters*, v. 23, p. 1151–1154.
- Ivy-Ochs, S., Schluchter, C., Kubik, P.W., Dittrich-Hannen, B., and Beer, J., 1995, Minimum ^{10}Be exposure ages of early Pliocene for the Table Mountain Plateau and the Sirius Group at Mount Fleming, Dry Valleys, Antarctica: *Geology*, v. 23, p. 1007–1010.
- Jouzel, J., and Merlivat, L., 1984, Deuterium and oxygen-18 in precipitation: Modeling of the isotopic effects during snow formation: *Journal of Geophysical Research*, v. 89, p. 11749–11757.
- Kurz, M.D., 1986, In situ production of terrestrial cosmogenic helium and some applications to geochronology: *Geochimica et Cosmochimica Acta*, v. 50, p. 2855–2862.
- Kurz, M.D., and Brook, E.J., 1994, Surface exposure dating with cosmogenic nuclides, in Beck, C., ed., *Dating in exposed and surface contexts*: Albuquerque, University of New Mexico Press, p. 139–159.
- Kyle, P.R., 1990, The McMurdo Volcanic Group—Western Ross Embayment, in LeMasurier, W.E., and Thomson, J.W., eds., *Volcanoes of the Antarctic plate and southern oceans*: American Geophysical Union Antarctic Research Series, v. 48, p. 19–134.
- Lachenbruch, A.H., 1961, Depth and spacing of tension cracks: *Journal of Geophysical Research*, v. 66, p. 4273–4292.
- Lachenbruch, A.H., 1962, Mechanics of thermal contraction cracks and ice-wedge polygons in permafrost: *Geological Society of America Special Paper 70*, p. 1–69.
- Lal, D., 1991, Cosmic ray labelling of erosion surfaces: In situ nuclide production rates and erosion models: *Earth and Planetary Science Letters*, v. 104, p. 424–439.
- Law, J., and van Dijk, D., 1994, Sublimation as a geomorphic process: A review: *Permafrost and Periglacial Processes*, v. 5, p. 237–249.
- Lewis, A.R., 2000, The paleoclimatic significance of massive buried glacial ice in Beacon Valley, Antarctica. [M.S. thesis]: Orono, University of Maine, 158 p.
- Mackay, J.R., 1980, Deformation of ice-wedge polygons, Garry Island, Northwest Territories: *Geological Survey of Canada Special Paper 80-1A*, p. 287–291.
- Mackay, J.R., 1993, Air temperature, snow cover, creep of frozen ground, and the time of ice-wedge cracking, western Arctic coast: *Canadian Journal of Earth Science*, v. 30, p. 1720–1729.
- Marchant, D.R., Denton, G.H., and Swisher, C.C., III, 1993a, Miocene-Pliocene-Pleistocene glacial history of Arena Valley, Quartermain Mountains, Antarctica: *Geografiska Annaler*, v. 75A, p. 269–302.
- Marchant, D.R., Denton, G.H., and Sugden, D.E., 1993b, Miocene glacial stratigraphy and landscape evolution of the western Asgard Range, Antarctica: *Geografiska Annaler*, v. 75A, p. 303–330.
- Marchant, D.R., Denton, G.H., Bockheim, J.G., Wilson, S.C., and Kerr, A.R., 1994, Quaternary ice-level changes of upper Taylor Glacier, Antarctica: Implications for paleoclimate and ice-sheet dynamics: *Boreas*, v. 23, p. 29–42.
- Marchant, D.R., Denton, G.H., Swisher, C.C., III, and Potter, N., Jr., 1996, Late Cenozoic Antarctic paleoclimate reconstructed from volcanic ashes in the Dry Valleys region, south Victoria Land: *Geological Society of America Bulletin*, v. 108, p. 181–194.
- McKay, C.P., Mellon, M.T., and Friedmann, E.I., 1998, Soil temperatures and stability of ice-cemented ground in the McMurdo Dry Valleys, Antarctica: *Antarctic Science*, v. 10, p. 31–38.
- Murton, J.B., Worsley, P., and Gozdzik, J., 2000, Sand veins and wedges in cold aeolian environments: *Quaternary Science Reviews*, v. 19, p. 899–922.
- Nishiizumi, K., Kohl, C.P., Arnold, J.R., Klein, J., Fink, D., and Middleton, R., 1991, Cosmic ray produced Be-10 and Al-26 in Antarctic rocks: Exposure and erosion history: *Earth and Planetary Science Letters*, v. 104, p. 440–454.

- Pechmann, J.C., 1980, The origin of polygonal troughs on the northern plains of Mars: *Icarus*, v. 42, p. 185–210.
- Péwé, T.L., 1959, Sand-wedge polygons (tessellations) in the McMurdo Sound region, Antarctica—A progress report: *American Journal of Science*, v. 257, p. 545–552.
- Phillips, W.M., McDonald, E.V., Reneau, S.L., and Poths, J., 1998, Dating soils and alluvium with cosmogenic ^{21}Ne depth profiles: Case studies from the Pajarito Plateau, New Mexico, USA: *Earth and Planetary Science Letters*, v. 160, p. 209–223.
- Pissart, A., 1990, Advances in periglacial geomorphology: *Zeitschrift für Geomorphologie*, v. 79, p. 119–131.
- Robinson, P.H., 1984, Ice dynamics and thermal regime of Taylor Glacier, south Victoria Land, Antarctica: *Journal of Glaciology*, v. 30, p. 153–160.
- Schäfer, J.M., Bauer, H., Denton, G.H., Ivy-Ochs, S., Marchant, D.R., Schlüchter, C., and Wieler, R., 2000a, The oldest ice on Earth in Beacon Valley, Antarctica: New evidence from surface exposure dating: *Earth and Planetary Science Letters*, v. 179, p. 91–99.
- Schäfer, J.M., Ivy-Ochs, S., Wieler, R., Leya, I., Bauer, H., Denton, G.H., and Schlüchter, C., 2000b, Cosmogenic noble gas studies in the oldest landscape on Earth: Surface exposure ages of the Dry Valleys, Antarctica: *Earth and Planetary Science Letters*, v. 167, p. 215–226.
- Schwerdtfeger, W., 1984, *Weather and climate of the Antarctic*: Amsterdam, Elsevier, 327 p.
- Shaw, J., 1976, Tills deposited in arid polar environments: *Canadian Journal of Earth Sciences*, v. 14, p. 1239–1245.
- Shaw, J., 1988, Sublimation till, in Goldthwait, R., and Matsch, C., eds., *Genetic classification of glacial deposits*: Rotterdam, A.A. Balkema, p. 141–142.
- Souchez, R.A., and Jouzel, J., 1984, On the isotopic composition in delta D and delta ^{18}O of water and ice during freezing: *Journal of Glaciology*, v. 30, p. 369–372.
- Stone, J.O., 2000, Air pressure and cosmogenic isotope production: *Journal of Geophysical Research*, v. 105, p. 23 753–23 759.
- Stone, J.O., Sletten, R.S., and Hallet, B., 2000, Old ice, going fast: Cosmogenic isotope measurements on ice beneath the floor of Beacon Valley, Antarctica: *Eos* (Transactions, American Geophysical Union), Fall Meeting Supplement, Abstract H52C–21.
- Stuiver, M., Denton, G.H., Hughes, T.J., and Fastook, J.L., 1981, History of the marine ice-sheet in West Antarctica during the last glaciation, a working hypothesis, in Denton, G.H., and Hughes, T.J., eds., *The last great ice sheets*: New York, Wiley Inter-science, p. 391–436.
- Sugden, D.E., Marchant, D.R., Potter, N., Jr., Souchez, Roland, Denton, G.H., Swisher, Carl C., and Tison, Jean-Louis, 1995, Miocene glacier ice in Beacon Valley, Antarctica: *Nature*, v. 376, p. 412–416.
- Summerfield, M.A., Stuart, F.M., Cockburn, H.A.P., Sugden, D.E., Denton, G.H., Dunai, T., and Marchant, D.R., 1999, Long-term rates of denudation in the Dry Valleys region of the Transantarctic Mountains, southern Victoria Land based on in situ produced cosmogenic Ne-21: *Geomorphology*, v. 27, p. 113–129.
- Swanson, D.K., Ping, C., and Michaelson, G.J., 1999, Diapirism in soils due to thaw of ice-rich material near the permafrost table: *Permafrost and Periglacial Processes*, v. 10, p. 349–367.
- Tschudi, S., 2000, *Surface exposure dating: A geologist's view with examples from both hemispheres* [Ph.D. dissert.]: Bern, Switzerland, University of Bern, 121 p.
- Ugolini, F.C., Bockheim, J.G., and Anderson, D.W., 1971, Soil development and patterned ground evolution in Beacon Valley, Antarctica, in *Permafrost Second International Conference*: Washington, D.C., National Academy of Sciences, p. 246–254.

MANUSCRIPT RECEIVED BY THE SOCIETY APRIL 19, 2001

REVISED MANUSCRIPT RECEIVED JANUARY 9, 2002

MANUSCRIPT ACCEPTED JANUARY 23, 2002

Printed in the USA